

論文 / 著書情報
Article / Book Information

題目(和文)	マンガン窒化物薄膜の成長と磁気特性に関する研究
Title(English)	Study on the Growth and Magnetism of Manganese Nitride Films
著者(和文)	李文暢
Author(English)	Wenchang Li
出典(和文)	学位:博士(工学), 学位授与機関:東京工業大学, 報告番号:甲第11769号, 授与年月日:2022年3月26日, 学位の種別:課程博士, 審査員:史 蹟,中村 吉男,木村 好里,林 幸,村石 信二
Citation(English)	Degree:Doctor (Engineering), Conferring organization: Tokyo Institute of Technology, Report number:甲第11769号, Conferred date:2022/3/26, Degree Type:Course doctor, Examiner:,,,,,
学位種別(和文)	博士論文
Category(English)	Doctoral Thesis
種別(和文)	要約
Type(English)	Outline

(博士課程)
Doctoral Program

論文要約

THESIS OUTLINE

系・コース : Department of, Graduate major in	材料 材料	系 コース	申請学位 (専攻分野)): Academic Degree Requested	博士 Doctor of (工学)
学生氏名: Student's Name	LI WENCHANG		指導教員 (主): Academic Supervisor(main)	史蹟
			指導教員 (副): Academic Supervisor(sub)	中村吉男

Study on the Growth and Magnetism of Manganese Nitride Films

Manganese nitride films are considered as potential functional materials due to the great variety of crystal structures, electronic, optical and magnetic properties. They are four stable phases depending on the nitrogen content at room temperature, including MnN, Mn₃N₂, Mn₂N, Mn₄N phases. **Tab.1** summarizes the magnetism and crystal structure of those four phases. Only Mn₄N shows the ferrimagnetism, and the others manganese nitrides show the antiferromagnetism. Mn₄N phase is face-centered cubic (FCC) structure, Mn₂N is hexagonal close-packed (HCP) structure, Mn₃N₂ and MnN phase are face-centered tetragonal (FCT) structure.

Tab.1 Magnetism and crystal structure of manganese nitride

Phase	Magnetism	Néel temperature (T_N)	Structure
MnN	Antiferromagnetism (AF)	650 K	FCT
Mn ₃ N ₂	Antiferromagnetism	925 K	FCT
Mn ₂ N	Antiferromagnetism	301 K	HCP
Mn ₄ N	Ferrimagnetism (FI)	738 K	FCC

Among them, MnN and Mn₄N have been paid more attention. The MnN film, as an excellent candidate of antiferromagnetic material, can be applied to the exchange bias (EB) effect to prepare magnetic memory devices due to the high Néel temperature, environmental safety and very low cost. The Mn₄N film, as the only ferrimagnetic phase among the manganese nitride, is mentioned to apply on current-induced domain wall motion (CIDWM) devices due to the low saturation magnetization, high spin polarization and perpendicular magnetic anisotropy (PMA). At present, the formation behaviors of

manganese nitrides are not explicit. The growth of Mn_4N film relies on the high-cost single crystal substrates, which restricts the further practical application. Moreover, the mechanism of perpendicular magnetic anisotropy is not fully understood. And the exchange coupling between MnN and ferromagnetic layers needs to be further investigated. The main research objectives of this study include three aspects: First, to study the formation of manganese nitrides films under different experimental conditions. Second, to obtain the large perpendicular magnetic anisotropy in Mn_4N films on glass substrate by improving the crystallinity of Mn_4N . Third, to understand the exchange coupling between MnN /ferromagnetic layer.

The outline of each chapter of this thesis is introduced as follows:

Chapter 1 Introduction: The research background, objectives, and organization of this thesis are presented. The background outlines the fundamental concepts and theories required to understand and discuss this thesis.

Chapter 2 Structure of manganese nitrides films and perpendicular magnetic anisotropy of Mn_4N films on glass substrate: This chapter first introduces the sample preparation and analyze techniques used in this thesis. And then the phase formation of manganese nitride films under different conditions is systematically studied. It tends to form the nitrogen-rich manganese nitride films under low substrate temperature (T_s) and high N_2 content ($N_2\%$) environment. On the contrary, high substrate temperature and low nitrogen environment obtain nitrogen-poor manganese nitride films (**Fig. 1**). Only the Mn_3N_2 film show strong crystallinity along (200) orientation, and the other manganese nitride films show poor crystallinity. Under appropriate experiment conditions ($N_2\% = 10-20\%$, $T_s = 200-300\text{ }^\circ\text{C}$, annealing temperature (T_a) = 200-500 $^\circ\text{C}$), the Mn_4N single layer film can be prepared with PMA (**Fig. 2**). The Mn_4N film exists in-plane tensile stress even it grows on glass substrate with amorphous surface. It is considered that Mn_4N films tend to form tetragonal structures in the growth to reach a minimum energy state. And the origin of PMA is considered to be the tetragonal distortion along c axis.

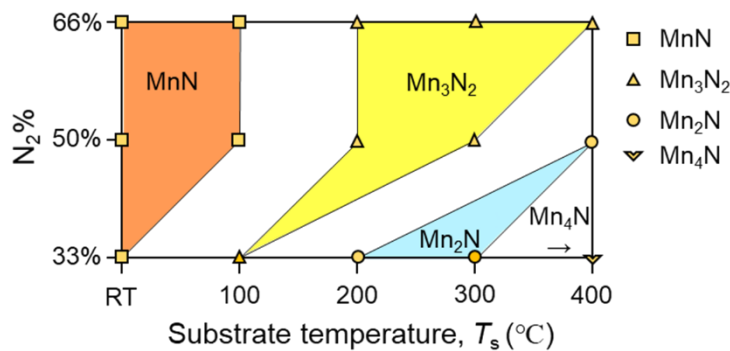


Fig. 1. Phase diagram with N_2 concentration ($N_2\%$) and substrate temperature (T_s)

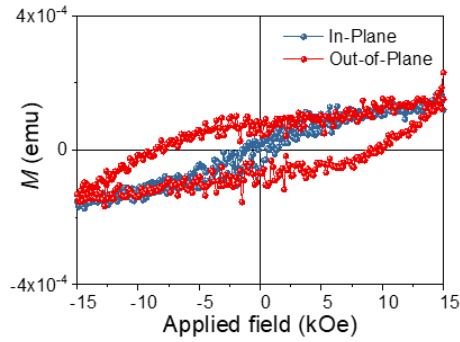


Fig. 2. Hysteresis loop of Mn_4N single layer with $\text{N}_2\%=10\%$, $T_s=250^\circ\text{C}$, $T_a=400^\circ\text{C}$.

Chapter 3 Enhancement of perpendicular magnetic anisotropy of Mn_4N films on glass substrate by Mn_3N_2 seed layer: To further improve the perpendicular magnetic anisotropy of Mn_4N films. Mn_3N_2 film is chosen as the seed layer to promote the growth of Mn_4N due to the same arrangement of Mn atoms of those two phases and the transition from Mn_4N to Mn_3N_2 only through the diffusion of nitrogen atoms (**Fig. 3**). Compared with Mn_4N single layer film directly deposited on glass substrate, the crystallinity and PMA of Mn_4N are significantly improved by inserting a Mn_3N_2 seed layer (**Fig. 4**). And Mn_3N_2 seed layer thickness (t_b) plays a crucial role in determining the structural and magnetic properties of Mn_4N (**Fig. 5**). The optimum seed layer thickness in the present work is from 16 to 24 nm. The Mn_3N_2 layer provides favorable nucleation sites for growing Mn_4N film and prevents Mn_4N from being oxidized by supplying N atoms through N diffusion (**Fig. 6**).

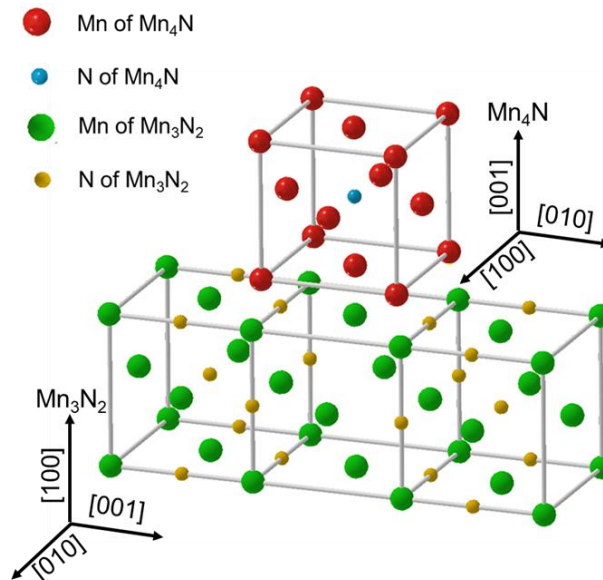


Fig. 3. Schematic diagram of Mn_4N (001) grows on the Mn_3N_2 (100).

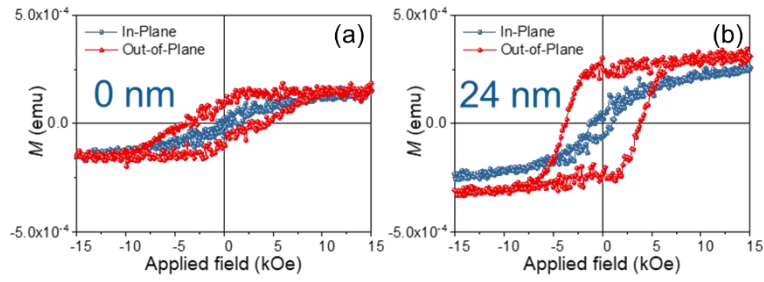


Fig. 4. The magnetization hysteresis loops of Mn_3N_2 (t_b nm)/ Mn_4N (45 nm) bilayer films: (a) $t_b = 0$ nm; (b) $t_b = 24$ nm.

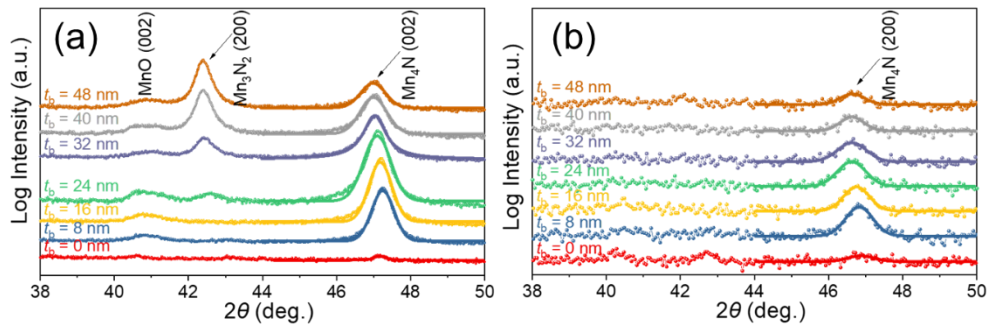


Fig. 5. Mn_3N_2 (t_b nm)/ Mn_4N (45 nm) bilayer films: (a) Out-of-plane XRD profiles; (a) In-plane XRD profiles.

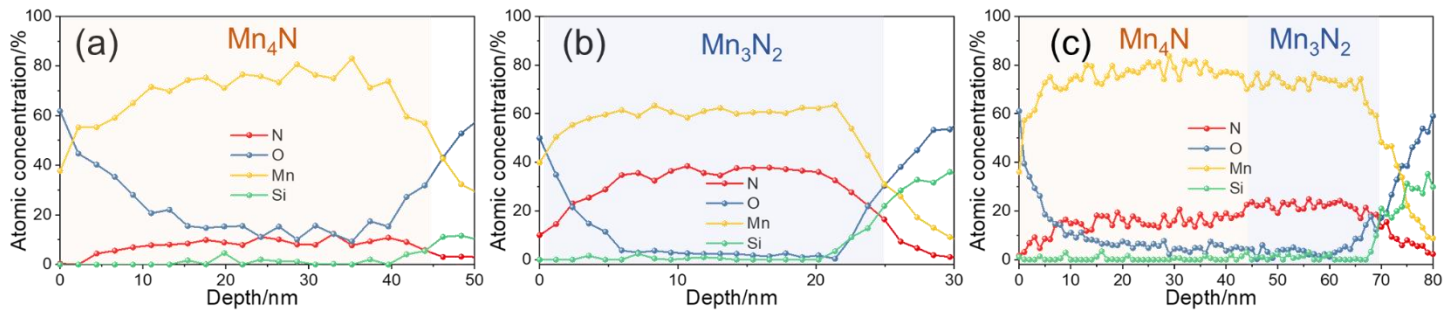


Fig. 6. XPS depth concentration profiles of (a) Mn_4N (45nm) single layer film; (b) Mn_3N_2 (24 nm) single layer film; (c) Mn_3N_2 (24 nm)/ Mn_4N (45 nm) bilayer film

Chapter 4 Epitaxial growth of Mn_4N film on MnO seed layer: In this chapter, another seed layer MnO is used to improve the PMA and crystallinity of Mn_4N . MnO has the same Mn atomics arrangement as Mn_4N , and the lattice mismatch between Mn_4N and MnO is around 12.5% which is close to the borderline (5-10%) of the perfect epitaxial growth (**Fig. 7**). Highly crystalline Mn_3N_2 film along (200) orientation will gradually be oxidized from the surface to the interior into the high crystalline MnO film along (001) orientation during the in-situ isothermal holding in the sputter atmosphere (**Fig. 8**). Epitaxial growth of Mn_4N on the MnO seed layer is realized with MnO [100](001) \parallel Mn_4N [100](001). Compared to the Mn_4N single layer film directly deposited on glass substrate, the crystallinity including the [001] preferred

orientation is greatly improved (Fig. 9).

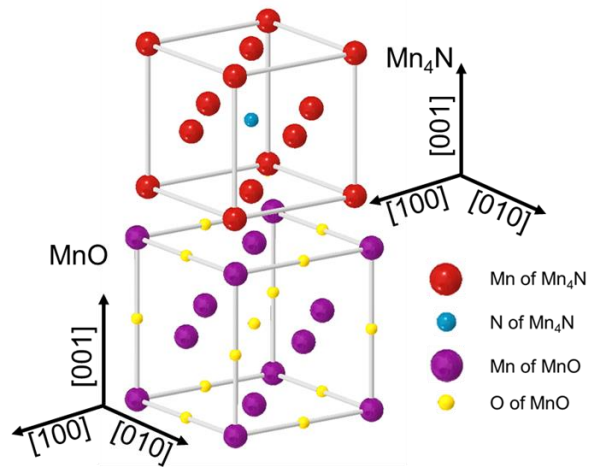


Fig. 7. Schematic diagram of Mn_4N (001) grows on the MnO (001).

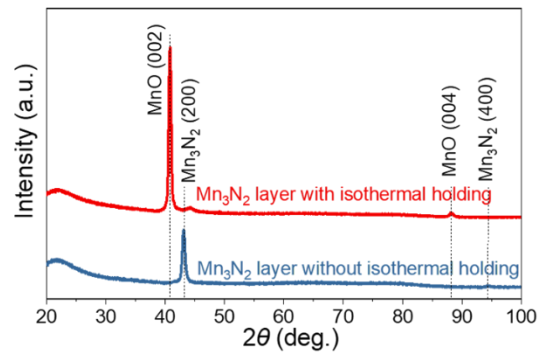


Fig. 8. XRD profiles of Mn_3N_2 (28 nm) single layer film with and without isothermal holding process.

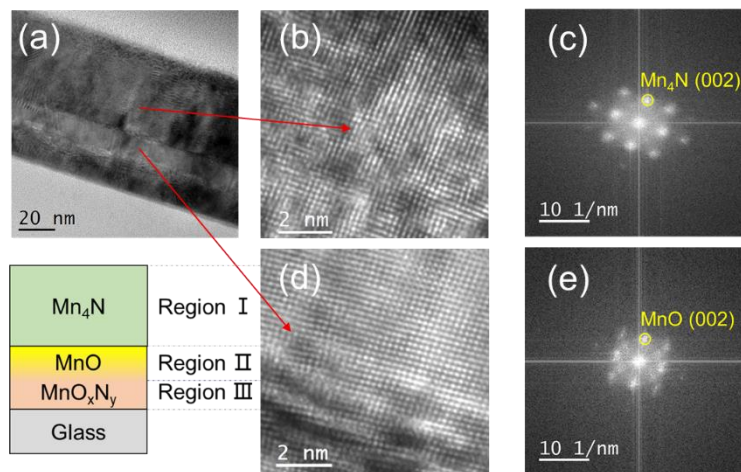


Fig. 9. TEM image of $\text{MnO}/\text{Mn}_4\text{N}$: (a) bright field image; (b) HRTEM image of the Mn_4N layer; (c) FFT image of the Mn_4N layer; (d) HRTEM image of the MnO layer; (e) FFT image of the MnO layer.

Chapter 5 Primitive exchange coupling in CoPt/MnN layered structures: In this chapter, the antiferromagnetic material MnN is used to establish exchange coupling with the ferromagnetic CoPt. And the primitive exchange bias which signifies exchange coupling occurred without field cooling has been observed. Primitive exchange coupling can be established at the interface between CoPt and MnN under a magnetic field as small as 6 Oe during deposition (**Fig. 10**). The interfacial spin configuration resulting in the exchange coupling is formed during the deposition of MnN on the surface of the magnetized CoPt layer (**Fig. 11**). The primitive exchange coupling shows similar constituting layer thickness dependence with the conventional field-cooling exchange coupling (**Fig. 12**).

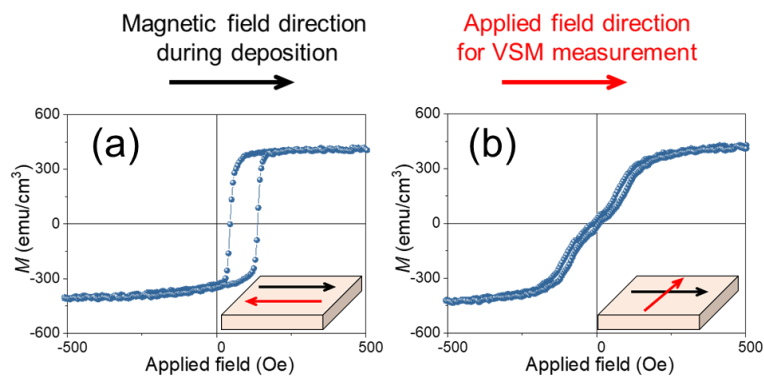


Fig. 10. The magnetization hysteresis loops of CoPt (4 nm)/MnN (50 nm) bilayer film measured with applied field along different in-plane directions: (a) The applied field direction is antiparallel to the direction of the field during deposition; (b) The applied field directions perpendicular to the direction of the magnetic field during deposition.

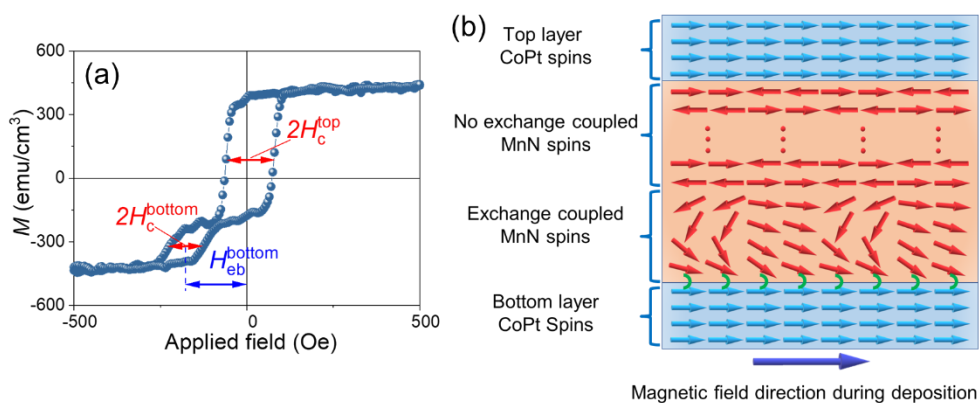


Fig. 11. (a) The magnetization hysteresis loops of CoPt (2 nm)/MnN (50 nm)/CoPt (5 nm) trilayer film; (b) Schematic diagram of the interfacial spin configuration for CoPt/MnN/CoPt trilayer film.

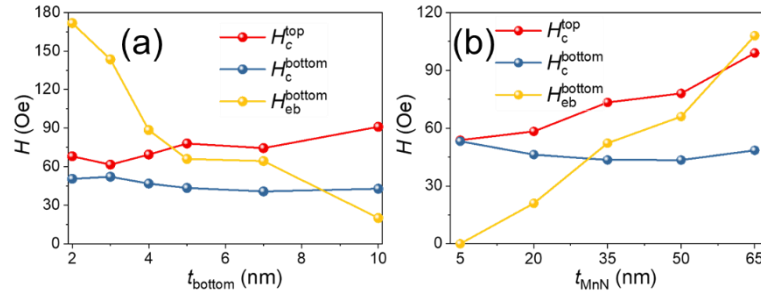


Fig. 12. (a) $H_{\text{eb}}^{\text{bottom}}$, H_c^{bottom} , and H_c^{top} dependence on t_{bottom} of [CoPt (5 nm)/MnN (50 nm)/CoPt (t_{bottom} nm)] trilayer films; (b) $H_{\text{eb}}^{\text{bottom}}$, H_c^{bottom} , and H_c^{top} dependence on t_{MnN} of [CoPt (5 nm)/MnN (50 nm)/CoPt (t_{MnN} nm)] trilayer films;

Chapter 6 General conclusions: The conclusions of this thesis are given.